Generator-coordinate spectra of $4n$ nuclei in d-s shell

S. B. Khadkikar and D. R. Kulkarni
Physical Research Laboratory, Ahmedabad 380009, India
(Received 1 April 1974)

The calculated energy spectra, quadrupole moments, and quadrupole transitions for $4n$ nuclei in d-s shell are reported. The framework of the generator coordinate method using angular momentum projected states from Hartree-Fock intrinsic states driven by an external quadrupole field is successfully employed. The agreement with experimental numbers is found to be quite satisfactory up to the middle of the d-s shell. The excited 0^+ levels and the electrical moments are satisfactorily explained.

[NUCLEAR STRUCTURE ^{20}Ne, ^{24}Mg, ^{28}Si, ^{32}S, ^{36}Ar; calculated levels J, q, $B(E2)$. Generator coordinate method; constrained Hartree-Fock.]

I. INTRODUCTION

It has been demonstrated[1] that the generator coordinate (GC) calculations performed with states projected on to the space of angular momentum from the Hartree-Fock (HF)[2] states driven by an external quadrupole field are indeed successful in accounting for most of the levels up to ~18 MeV excitation in the ^{20}Ne nucleus. These were also in excellent agreement with the exact shell-model results employing the same effective interaction. Thus we were encouraged to investigate energy spectra and electromagnetic properties of all $4n$ nuclei in d-s shell using this method. This is indeed desirable because the exact shell-model calculations and its results become rapidly lengthy and get involved as the number of valance nucleons to be treated increases. Also, it is felt, we understand more about the structure of these rather low-lying nuclear levels if we can attribute them with a few intrinsic states.

We have performed calculations to obtain isospin $T=0$ states of ^{20}Ne, ^{24}Mg, ^{28}Si, ^{32}S, and ^{36}Ar using an interaction given by Preedom and Wildenthal[3] obtained by empirical modification of Kuo's interaction so as to achieve a best fit for the levels of nuclei in the mass range $A=18$–22. By their very nature, these matrix elements are expected to give good results up to the middle of d-s shell. We, however, extended their use in the later part of the d-s shell. Even though very satisfactory results are not obtained in the later part of d-s shell, we have understood the deficiencies of the matrix elements in this region in the light of the results obtained. The "hole" spectrum of ^{40}Ca which gives the excitation spectrum of ^{39}Ca or ^{39}K should be fitted with the effective interaction to obtain agreement in the later part of the d-s shell.

The HF state driven by an external quadrupole field λQ_0^2 incorporates all the collective states connected by quadrupole transition amplitudes. The HF iteration procedure by itself gives only the local minima. Hence we see a shape transition at a particular value of λ for all nuclei. The nature of the kernels between these transition is rather uncertain[1] and would depend upon the method[4,5] one may use to obtain the intermediate solutions. It is our contention that a reasonably good description of the low-lying levels in the nuclear spectra is possible without incorporating the intermediate kernel which represents moreover, local maxima in a HF calculation. The theory of the collective motion in Hartree-Fock formalism has been discussed by Villars.[6] It is shown that a certain mass parameter for the quadrupole excitations can be defined and the value of this parameter is not affected if one stabilizes[4] the driving procedure by the addition of the term $\frac{1}{2}\gamma_0\langle Q\rangle^2$ to the expectation value of the Hamiltonian. Here, the parameter $\gamma_0>0$ and $\langle Q\rangle$ is the expectation value of the driving field. Hence in our calculations we have included only those points which correspond to local minima.

After giving a rather brief resume of the method we shall discuss the results of each nucleus separately.

II. METHOD OF CALCULATION

The actual method of calculations is exactly the same as that described in the earlier paper.[1] We minimize the free energy $E=\langle\psi_\lambda|H-\lambda Q_0^2|\psi_\lambda\rangle$ in the HF procedure to obtain the states $|\psi_\lambda\rangle$. The Hill-Wheeler integral equation[7] with the coordinate λ is solved approximately for states of good angular momentum projected from the states $|\psi_\lambda\rangle$. The Hill-Wheeler integral equation is approximated by a matrix equation by discretizing the coordinate λ as follows:

$$\sum_m (H^J_{n,m}-E^J I^J_{n,m}),\quad f_m=0\,. \tag{1}$$

These equations are solved by usual orthonormalization diagonalization procedure.

In these calculations for the d-s shell nuclei we assume an inert ^{16}O core outside which there are certain number of valence nucleons. The valence nucleons are distributed among the single particle states whose energies are taken from ^{17}O spectrum. $\epsilon d_{5/2} = 0$, $\epsilon s_{1/2} = 0.87$, and $\epsilon d_{3/2} = 5.08$ under the influence of an effective interaction whose matrix elements are those given by Preedom and Wildenthal.[3] We carry HF calculations with this Hamiltonian for the $4n$ nuclei. We found for almost all the nuclei axially deformed HF solutions are lowest except for ^{24}Mg which has triaxial shape and for ^{32}S which is spherical. These results are displayed in Table I.

We have chosen the lowest axially symmetric (or spherical) solutions and have driven these with the help of an external quadrupole field in a HF procedure. Our main aim in these calculations is to understand the nature of the levels next to lowest "band," in particular the excited 0^+ level. We have varied the number of points to be used in solving the Eq. (1) until we find that there is no significant variation in the position of the lowest levels. The wave functions obtained consist of good angular momentum states projected from a linear combination of intrinsic states. These are used to compute electric quadrupole moments (Q_e) and the reduced electric quadrupole transitions $B(E2)$ for various low-lying states. We compare our results with exact shell model calculations wherever they are available and with the experimental results.

III. RESULTS AND DISCUSSION

^{20}Ne

The response of the HF states to the external quadrupole driving field is shown in the Fig. 1, in

TABLE I. The energy (E HF), the mass quadrupole moments $\langle Q_0^2 \rangle$ and $\langle Q_2^2 \rangle$ of the Hartree-Fock states for $4n$ nuclei in d-s shell.

Nucleus	E HF (MeV)	$\langle Q_0^2 \rangle$ (b^2)	$\langle Q_2^2 \rangle$ (b^2)
^{20}Ne	−20.01	15.31	0
	−13.53	−8.00	0
^{24}Mg	−47.05	17.60	0
	−39.76	−15.34	0
	−48.22	18.46	5.14
^{28}Si	−74.61	22.72	0
	−82.01	−19.81	0
^{32}S	−114.63	0	0
^{36}Ar	−142.73	6.66	0
	−142.75	−9.45	0
	−142.67	6.24	4.23
^{40}Ca	−167.80	0.0	0.0

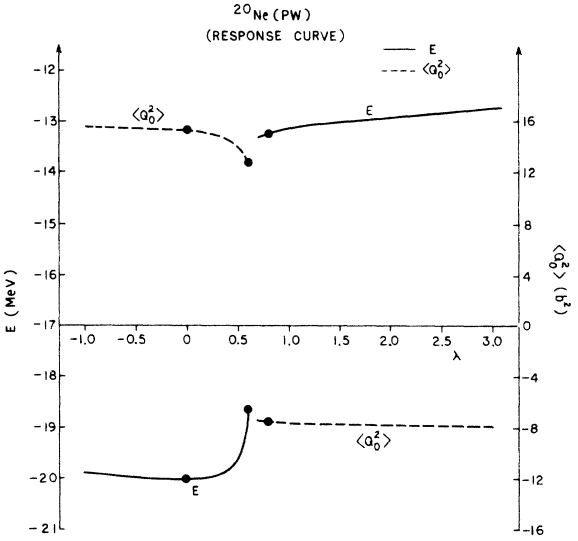

FIG. 1. The response curve for ^{20}Ne obtained as the variation of Hartree-Fock energy E (solid-line curve) and that of quadrupole moment $\langle Q_0^2 \rangle$ (dashed-line curve) with λ. Both the curves are drawn in arbitrary units. The circled points are used in GC calculations.

which we have plotted the intrinsic energy (E) and the mass quadrupole moment (Q) against the strength of the external quadrupole field (λ). These curves for the Preedom-Wildenthal (PW) interaction are quite similar to those obtained[1] with Kuo interaction. However the HF solution at $\lambda = 0$ is less deformed and hence the nucleus is softer in the prolate side. The points included in the generator-coordinate (GC) calculations are indicated by circles on the response curves. The three-point approximation gives an energy spectrum shown in the Fig. 2. The first excited 0_2^+ state

TABLE II. The reduced $B(E2)$ for the transition $J_i \to J_f$ (in e^2 fm^4) and the charge quadrupole moments $\langle Q_0^2 \rangle$ for the states J_i (in e fm^2) for $T = 0$, positive parity of states of ^{20}Ne are given along with the shell-model results and the experimental values.

J_i	J_f	Calculated	Shell model[a]	Experimental[a]
2_1	0_1	48.16	48.1	57 ± 8 96 ± 14
4_1	2_1	59.12	59.7	49.7 ± 4.5
6_1	4_1	48.09	48.8	89.8 ± 19.2
8_1	6_1	28.14		
0_2	2_1	5.4		
2_1		−14.33	−14.3	−21 ± 3
4_1		−17.63		
6_1		−19.01		
8_1		−18.86		

[a] Halbert *et al.*, 1971 (Ref. 9).

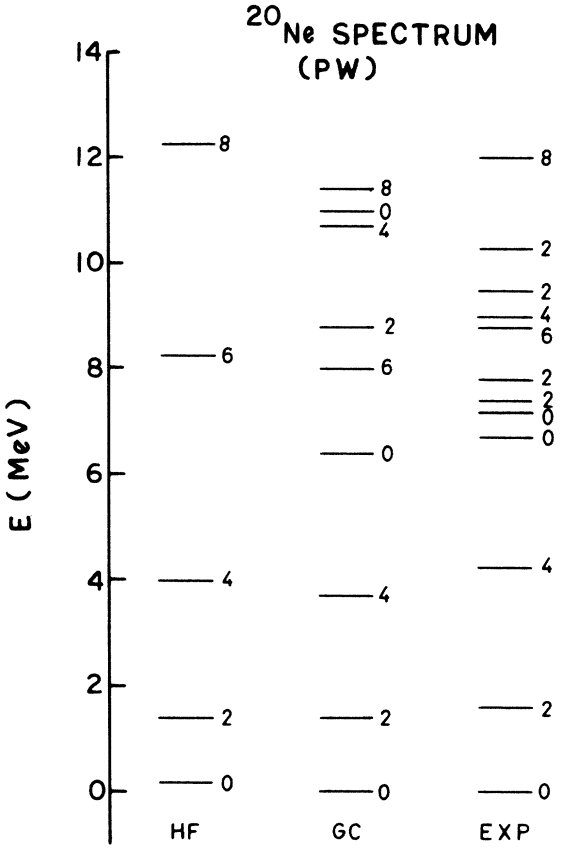

FIG. 2. Energy spectrum of ^{20}Ne. The results of projected Hartree-Fock (HF) and the generator-coordinate (GC) calculations are compared with the experimental (EXP) results

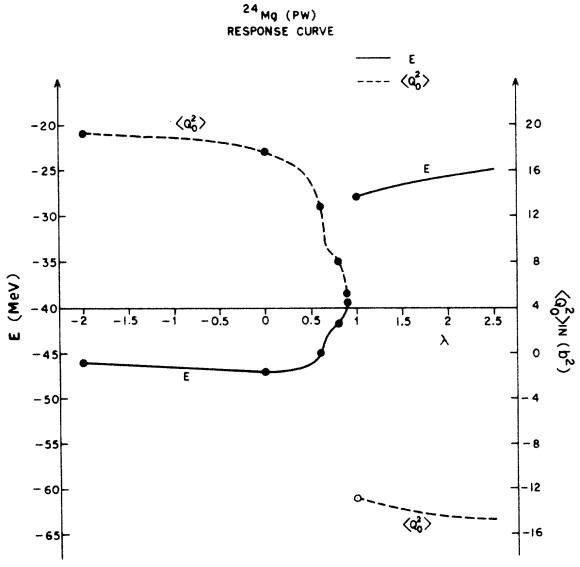

FIG. 3. Response curve for ^{24}Mg (for details see caption of Fig. 1).

obtained compares very well with the experimental levels, while the 4_1^+, 6_1^+, and 8_1^+ levels are lowered compared with the simple HF projection results.

The calculated $B(E2)$ values (see Table II) are less than the experimental values. The charge quadrupole moment of the first excited 2_1^+ state (see Table II) is also less than the experimental value.[8] However, these values are quite close to those obtained in an exact shell-model calculation[9] with Kuo's interaction matrix elements[10] with effective charges $e_p = 1.5$, $e_n = 0.5$, which are also the values used throughout the present calculations. The ground band remains essentially the HF-projected state, while the excited 0_2^+ state has very small overlap with the 0_1^+ state obtained from the HF state at $\lambda = 0$. Thus $0_2^+ \rightarrow 2_1^+$ transition rate is small.

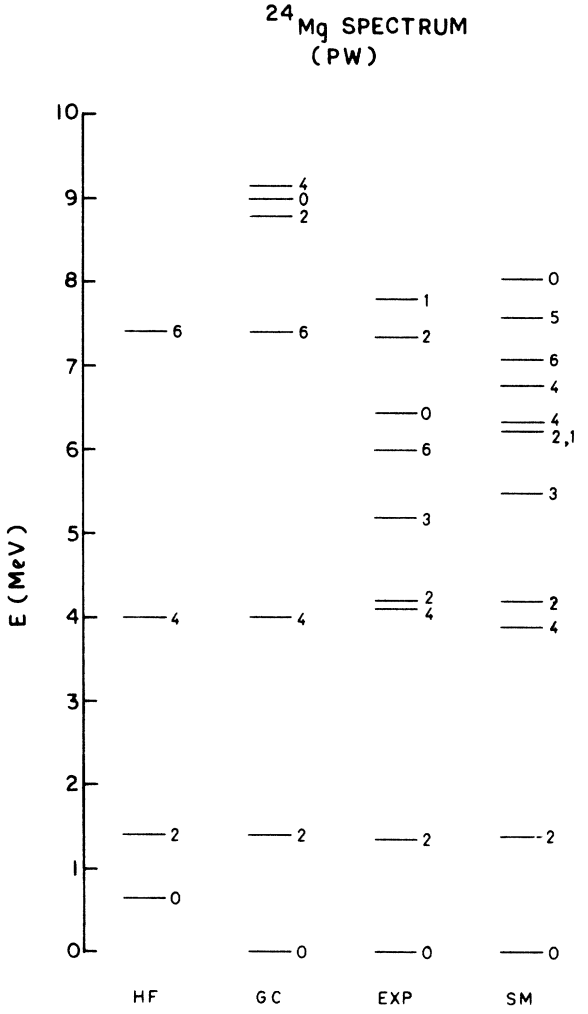

FIG. 4. Energy spectrum of ^{24}Mg. The results of projected Hartree-Fock (HF) and the generator-coordinate (GC) calculations are compared with the experimental (EXP) and the shell-model (SM) results.

TABLE III. The reduced $B(E2)$ for the transition $J_i \rightarrow J_f$ (in e^2 fm^4) and the charge quadrupole moments $\langle Q_0^2 \rangle$ for the states J_i (in e fm^2) for $T=0$, positive parity states of ^{24}Mg are given along with the shell-model results and the experimental values.

J_i	J_f	Calculated	Shell model [a]	Experimental [a]
2_1	0_1	70.66	63.00	89 ±10
4_1	2_1	97.32		
6_1	4_1	94.51		
8_1	6_1	75.36		
2_1		−17.36	−16.00	−24.3± 3.5
4_1		−21.58		
6_1		−21.73		
8_1		−19.83		

[a] McGrory and Wildenthal, 1971 (Ref. 12).

TABLE IV. The reduced $B(E2)$ for the transition $J_i \rightarrow J_f$ (in e^2 fm^4) and the charge quadrupole moments $\langle Q_0^2 \rangle$ for the states J_i (in e fm^2) for $T=0$, positive parity states of ^{28}Si are given along with the shell-model results and the experimental values.

J_i	J_f	Calculated	Shell model [a]	Experimental [a]
2_1	0_1	94.76	89.74	61 ±20 74 ± 8
4_1	2_1	137.75	118.01	79 ±11 48 ±11 96 ± 8
6_1	4_1	134.91	98.12	67 ±36 111 ±56
0_2	2_1	55.9	28.29	48 ±15
2_2	2_1	5.86	12.21	7.7 ± 3.5 9.6 ± 4.6 13.6 ± 9.1
4_2	2_1	1.20	0.02	3.8 ± 0.9 5.3 ± 1.3
2_2	0_1	0.04	0.13	0.91± 0.6 1.26± 0.66 2.8 ± 1.5
2_1		20.49		16 ± 5
4_1		25.90		
6_1		28.41		

[a] Soyeur and Zucker, 1972 (Ref. 13).

^{24}Mg

The HF results for this nucleus show that the triaxial[11] solution is lowest (see Table I), but it is only slightly lower than the prolate solution. The GC calculations by driving the triaxial solution to different deformations with different triaxial distortions would be desirable. But this would be rather complicated and since the axial solution is quite low, we felt that the results obtained by using the axial solutions would be quite reasonable especially for 0^+ states. Hence we carried out calculations for the axially symmetric prolate solution. The intrinsic state is quite soft on the prolate branch (Fig. 3) and we chose six points on this curve for the GC calculation. The calculated energy spectrum (see Fig. 4) is compared with the shell-model spectrum.[12] The agreement is quite good for the ground state band and the excited 0_2^+ state, thus justifying our approximation. However,

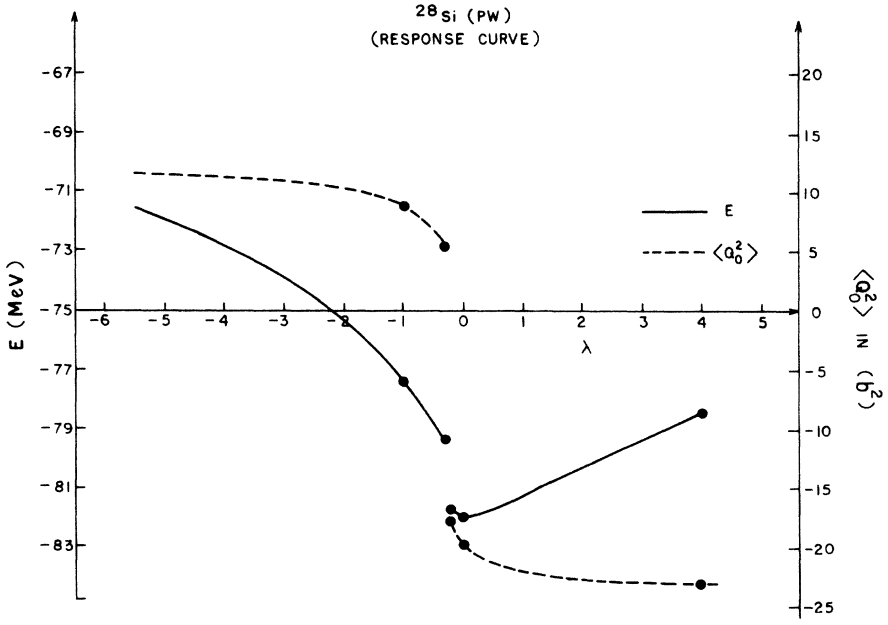

FIG. 5. Response curve of ^{28}Si (for details see caption of Fig. 1).

TABLE V. The reduced $B(E2)$ for the transition $J_i \to J_f$ (in e^2 fm^4) and the charge quadrupole moments $\langle Q_0^2 \rangle$ (in e fm^2) for the states J_i for $T=0$, positive parity states of ^{32}S are given along with the shell-model results and the experimental values.

J_i	J_f	Calculated	Experimental [a]
0_1	2_1	118.34	200 ±22
2_1	4_1	132.30	106. ±19
4_1	6_1	93.32	
6_1	8_1	52.38	
0_1	2_2	69.90	39.8± 3 67.5± 8 70 ±30
0_2	2_1	182.40	141 ±36
2_2	2_1	15.50	52
2_1		−13.72	−16 ± 6
4_1		−16.46	
6_1		−14.63	
8_1		−4.92	

[a] Wildenthal *et al.*, 1971 (Ref. 14).

the agreement between the calculated and the experimental spectra is not as good for the 6_1^+ and 8_1^+ levels because the observed states are quite low compared with the calculated positions. It is noted that compared with the simple HF projection, $0_1^+ \to 2_1^+$ separation is considerably improved.

The success of axially symmetric solution for $J=0$ states can be understood qualitatively in the following way. As far as $J=0$ states are concerned, even in the triaxial solution only the $K=0$ part of the triaxial solution contributes. In the present calculations we deal with the $K=0$ bands obtained by driving the lowest prolate HF solution by an external quadrupole field. In other words the correlations introduced in the axial GC calculations can compensate for the axial approximation if the triaxial modification is small. This is true of the ^{24}Mg calculations with PW interaction as the axial and the triaxial HF states have very large overlap (≈90%) and the triaxiality is small as seen from table I.

The reduced $B(E2)$ and the charge quadrupole moment of the 2_1^+ state (see Table III) are only slightly underestimated as compared with the experimental values.[8] The ground state 0_1^+ which arises mainly from the $\lambda=0$ HF state has large correlations from states at other λ values leading to an improvement in $0_1^+ \to 2_1^+$ separation, while the lowest 2_1^+, 4_1^+ states are little affected.

^{28}Si

In the case of ^{28}Si the response curve (Fig. 5) is quite soft even though the quadrupole moment does not change very much on the oblate side. In all we have included five points in our final calculation as shown in the Fig. 5. It is seen from Fig. 6 that we obtain very good agreement for the ground state 0_1^+, 2_1^+, and 4_1^+ states as well as the excited 0_2^+ state as compared with the experiment and the shell-model calculations[13] employing, however, a different interaction and configuration space.

As far as the reduced transition probabilities (see Table IV) are considered we obtain quite good

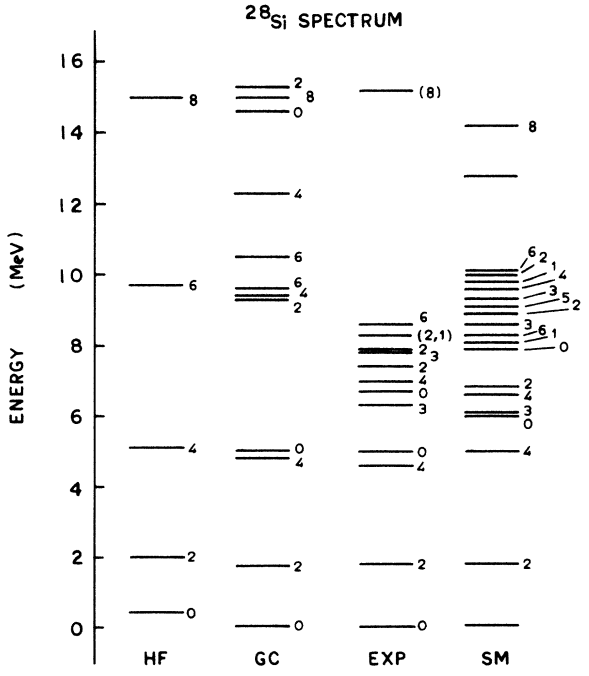

FIG. 6. Energy spectrum of ^{28}Si (for details see caption of Fig. 4).

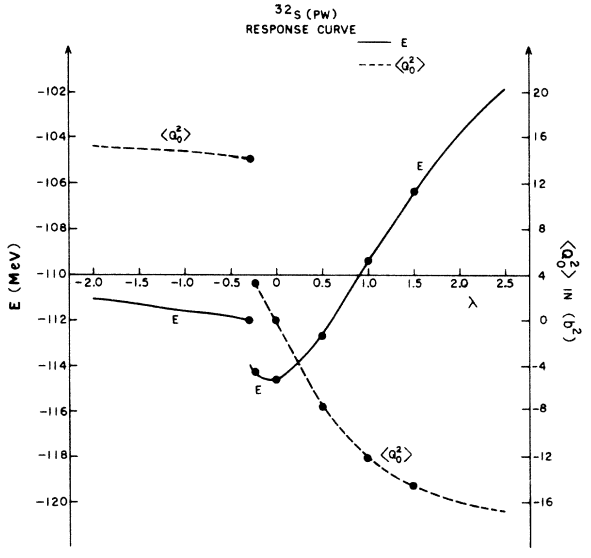

FIG. 7. Response curve of ^{32}S (for details see caption of Fig. 1).

agreement with the experimental values. In particular, the $0_2^+ \rightarrow 2_1^+$ transition rate is much better than the shell-model value as compared with the experimental result. It should be noted that for the same effective charges we are overestimating the transition rates in contradiction with the earlier nuclei in d-s shell. The lowest 0_1^+, 2_1^+, and 4_1^+ states are ($\lambda = 0$) HF-projected states with significant mixing from other states, while next excited 0_2^+, 2_2^+ states have little overlap with $\lambda = 0$ HF-projected states. The significant transition strength for $0_2^+ \rightarrow 2_1^+$ transition comes essentially through the amplitudes of the states at $\lambda = 0.3$ and -1.0 in the 2_1^+ state. The quadrupole moment of 2_1^+ state agrees quite well with the experimental value.[8]

^{32}S

The only HF solution found is spherical in shape corresponding to the full occupation of $d_{5/2}$ and $S_{1/2}$ levels. This solution when driven has a quite soft response on oblate branch of the response curve (see Fig. 7) while there is a sudden shape transition on the prolate side. The prolate state after the transition is quite stiff. Hence in the GC calculation five points on the spherical-oblate branch of the response curve were necessarily included, while a single point on the prolate branch was enough. The resulting energy spectrum (see Fig. 8) gives the position of excited 0_2^+ state quite satisfactorily, while the rest of the levels are quite spread out compared with the experimental level spacing. It is possible that this is a defect of the effective interaction which also gives quite large spacing for the "holes" in ^{40}Ca as compared with experimental ^{39}K spectrum (see Table VII). However, the reduced transition rates $B(E2)$ and the static quadrupole moment of the excited 2_1^+ state are in reasonable agreement (Table VII) with the experimental values.[8] In particular, we get $B(E2)$ for the 0_2 to 2_1 transition in good agreement with the experimental value contrasted with the shell-model results[14] (obtained by using different interactions) which are underestimated considerably (46 to 27 e^2fm^4). We obtain somewhat less $B(E2)$ for the $0_1^+ \rightarrow 2_1^+$ transition compared with the experimental value. The calculations for the nuclei ^{28}Si and ^{32}S which are in the middle of the d-s shell are quite sensitive to the nature of the effective interaction. Even a slight change in some of the matrix elements may lead to a sudden change in shape of the ground HF solution. As it is, it should be noted that we obtain a quite satisfactory result for the quadrupole moment of the excited 2_1^+ state. The 0_1^+ ground state has a overlap of 0.883 with the spherical HF state at $\lambda = 0$ and 0.649 with the very deformed state at $\lambda = -0.28$ after the

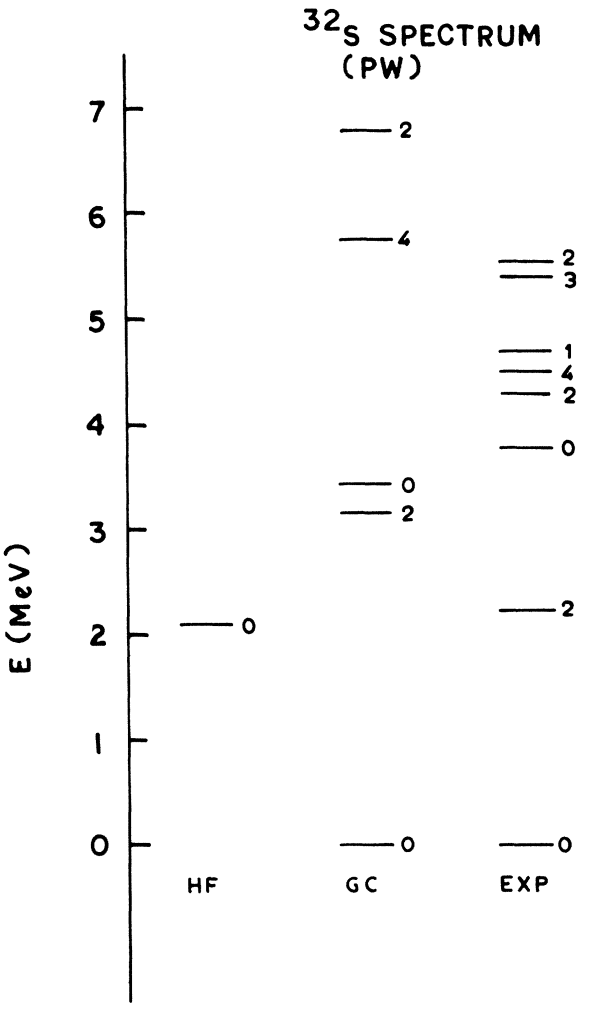

FIG. 8. Energy spectrum of ^{32}S (for details see caption of Fig. 2).

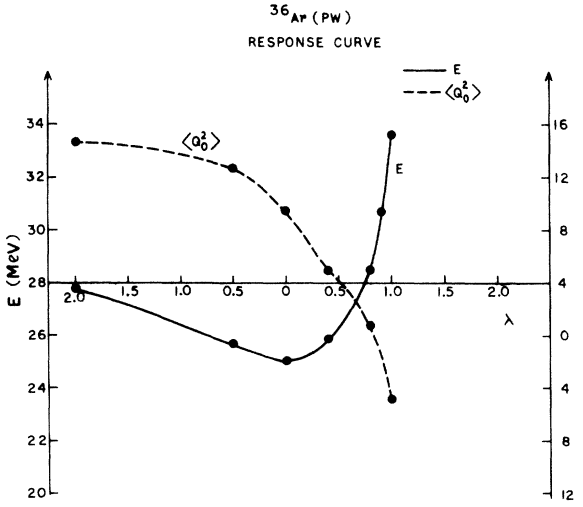

FIG. 9. Response curve of ^{36}Ar (for details see caption of Fig. 1).

TABLE VI. The reduced $B(E2)$ for the transition $J_i \rightarrow J_f$ (in e^2 fm^4) and the charge quadrupole moment $\langle Q_0^2 \rangle$ for the states J_i (in e fm^2) for $T=0$, positive parity states of ^{36}Ar are given along with the experimental values.

J_i	J_f	Calculated	Experimental [a]
2_1	0_1	46.61	68 ±17
4_1	2_1	31.83	75 ±12
6_1	4_1	17.95	
2_2	0_1	3.11	2.88± 0.98
2_2	2_1	13.40	40 ±13
2_1		12.60	16 ± 6
4_1		5.05	
6_1		18.81	

[a] Moinster and Alfred, 1970 (Ref. 15).

shape transition. The excited 0_1^+ state has overlaps of −0.320 with the $\lambda=0$ HF state and 0.748 with the $\lambda=-0.28$ state. The collectivity signaled by large $B(E2)$ transition rates is thus shared by the two 0^+ states through the mixing of the deformed and spherical shapes.

^{36}Ar

The oblate shaped HF solution for ^{36}Ar has quite a smooth response to the external quadrupole field as seen from the response curve (Fig. 9) which has no sudden transition. We included in all five points in our final GC calculation when the final results were considerably stabilized. The calculated levels (see Fig. 10) are too sparse even though the ground "band" ($0_1^+, 2_1^+, 4_1^+$) is rather compressed. Excitations across the d-s shell might become quite important at the end of this shell and these may lead to a considerable change in the excitation spectrum. However, in general, the calculated $B(E2)$ values and the quadrupole moment of excited 2_1^+ state (see Table VI) are in good agreement with the experimental results.[8,15]

We have also carried out HF calculation for ^{40}Ca nucleus in which the s-d shell is fully occupied (see Table I). The HF single particle energies for the occupied orbitals also give the excitation spectrum for the nucleus with one nucleon less, such as ^{39}K or ^{39}Ca. We see (Table IV) that the $d_{3/2} - S_{1/2}$ hole separation is 6.51 MeV, much larger than that in ^{39}K spectrum (2.53 MeV). This may be due to the fact that the interaction matrix elements in the $(d_{3/2})^2$ and $(d_{3/2}S_{1/2})$ states are weak. A suitable change in the center of gravity of the matrix elements in these states leads to a correct separation. However, when the interaction thus modified is employed in HF and projection calculation, it generates deformed ^{32}S and a more formed ^{36}Ar HF states giving rise to much more compressed spectra. A more extensive search for the interaction which would give better energy spectra without drastically changing the nature of the wave function is needed. Efforts are in progress in this direction within the framework of the present model.

TABLE VII. Energy spectrum of ^{39}K.

State	Calculated (MeV)	Experimental (MeV)
$\frac{3}{2}$	0	0
$\frac{1}{2}$	6.51	2.53
$\frac{5}{2}$	14.65	

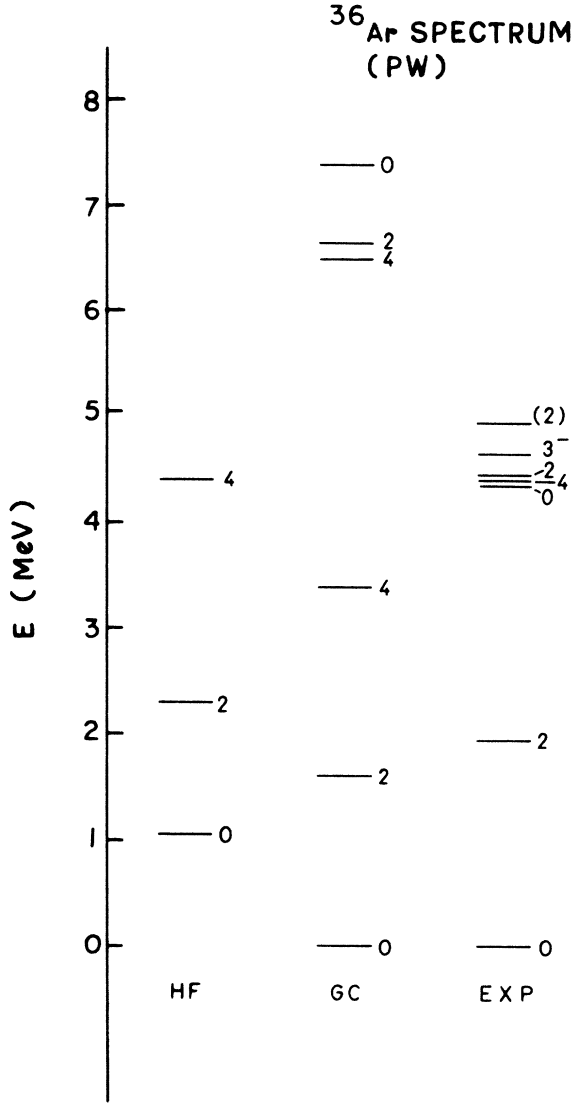

FIG. 10. Energy spectrum of ^{36}Ar (for details see caption of Fig. 2).

IV. CONCLUSION

The generator coordinate method is applied to $4n$ nuclei in d-s shell. Even these simple nuclei display all types of shapes and the transitions among these shapes in low-lying states. We have been able to obtain the structure information for the low-lying states of $4n$ nuclei in d-s shell in terms of few intrinsic states generated from a response to the quadrupole field. This in itself is a more transparent way than the complex shell-model calculations to understand the structure of nuclei. We see that the first excited 0_1^+ state is a state belonging to the transition from one shape to another in the sense that we invariably found that the simplest way to obtain this state is to include the transition point in the GC calculations. We have also been able to point out certain desirable changes which should be made in the matrix elements, based on the results of our present calculation. Efforts are in progress to see if, indeed, there is a single effective interaction in the d-s shell region that makes it possible to obtain a certain uniform degree of agreement between the calculated and the observed spectra, and the transition rates and the moments of all the nuclei.

[1]S. B. Khadkikar and D. R. Kulkarni, Phys. Rev. C 6, 866 (1972).

[2]For unconstrained HF and HF projection calculations in d-s shell see I. Kelson, Phys. Rev. 110, 2189 (1963); I. Kelson and C. A. Levinson, *ibid.* 134, B268 (1964); W. H. Bassichis, B. Giraud, and G. Ripka, Phys. Rev. Lett. 15, 980 (1965); M. R. Gunye and C. S. Warke, Phys. Rev. 156, 1087 (1969); and also see the review by G. Ripka, in *Advances in Nuclear Physics*, edited by M. Baranger and E. Vogt (Plenum, New York, 1968), Vol. I.

[3]B. M. Preedom and B. H. Wildenthal, Phys. Rev. C 6, 1633 (1972).

[4]B. Giraud, J. Le Tourneux, and S. K. M. Wong, Phys. Lett. 32B, 23 (1970).

[5]W. H. Bassichis and L. Wilets, Phys. Rev. Lett. 22, 799 (1969); 27, 1451 (1971).

[6]F. M. H. Villars, in *Dynamic Structure of Nuclear States*, edited by D. J. Rowe *et al.* (Univ. Toronto Press, Toronto, 1972).

[7]D. L. Hill and J. A. Wheeler, Phys. Rev. 89, 1102 (1953).

[8]K. Nakai, F. S. Stephens, and R. M. Diamond, Phys. Lett. 34B, 389 (1971).

[9]E. C. Halbert, J. B. McGrory, B. H. Wildenthal, and S. P. Pandya, in *Advances in Nuclear Physics*, edited by M. Baranger and E. Vogt (Plenum, New York, 1971), Vol. 4.

[10]T. T. S. Kuo, Nucl. Phys. A103, 71 (1967).

[11]J. Bar-Touv and I. Kelson, Phys. Rev. 138, 1035 (1965).

[12]J. B. McGrory and B. H. Wildenthal, Phys. Lett. 34B, 373 (1971).

[13]M. Soyeur and A. P. Zucker, Phys. Lett. 41B, 135 (1972).

[14]B. H. Wildenthal, J. B. McGrory, E. C. Halbert, and H. D. Graber, Phys. Rev. C 4, 1708 (1971).

[15]M. A. Moinster and W. P. Alfred, Nucl. Phys. A145, 143 (1970).